Chemical Science

Accepted Manuscript

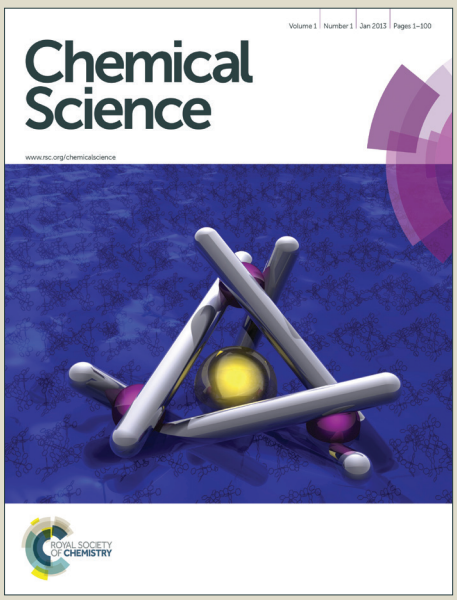

ROYAL SOCIETY OF CHEMISTRY

www.rsc.org/chemicalscience

Chemical Science

RSCPublishing

ARTICLE

Reversible Assembly of Enantiomeric Helical Polymers: From Fibers to Gels

Cite this: DOI: 10.1039/xoxxoooooox

Seila Leiras, Félix Freire,* Emilio Quiñoá, Ricardo Riguera*

Received ooth January 2012,
Accepted ooth January 2012

DOI: 10.1039/xoxxoooooox

www.rsc.org/

A novel class of stereocomplex is described by interaction of helically complementary poly(phenylacetylene)s (PPAs) carrying a α-methoxy-α-trifluoromethylphenylacetamide group as pendant. The stereocomplex formation requires the presence of *cis* amide bonds on the polymer external crest to provide efficient cooperative supramolecular hydrogen bonding between matching enantiomeric helical structures. Interlocking of the chains gives rise to supramolecular fiber-like aggregates that at higher concentrations results in gels. Modification of the *cis-trans* amide conformation at the pendants allows the controlled formation and cleavage of the stereocomplex due to a dramatic change between intermolecular and intramolecular hydrogen bond interactions.

Introduction

Stereocomplexes are supramolecular entities formed by the interaction of complementary stereoregular polymers generating a new material with different properties in comparison with the parent polymers.[1, 2]

Well known examples of homo-stereocomplexes are those formed by the association of an isotactic with a syndiotactic polymer —for instance poly(methylmetacrylate)s (*it*- and *st*-PMMA)—,[3] by the interaction between two enantiomeric polymers —*e.g.* poly-*D*- and poly-*L*-(lactic acid) (PLA)—,[4] or those made from some polypeptides —*D*- and *L*-amino acids—[5] and polyamides —e.g. *D*- and *L*-poly(hexamethylene di-*O*-methyltartaramide)s—.[6]

The formation of the stereocomplexes requires two complementary scaffolds, which are linked together through supramolecular interactions. Those made from PMMA and PLA have been amply studied during the last decades showing that the existence of stereoselective Van der Waals forces is crucial for the stabilization of the PMMA stereocomplexes, while those from PLA seem to be stabilized by weak hydrogen bond interactions.[7]

In this paper we describe a new class of homo-stereocomplex (fiber-like aggregates and gels) made by the interaction of helically complementary poly(phenylacetylene)s (PPAs)[8] stabilized by cooperative supramolecular hydrogen-bonding among *cis* amide groups located on the polymer crest. We will show also that the formation of the stereocomplex is highly specific for the *cis* conformer and its cleavage can be conveniently tuned by interaction with solvents that modify the *cis-trans* amide equilibria at the pendants —and as a result, the inter- and intramolecular hydrogen bond interactions—. This is, to our knowledge, the first example of a stereocomplex that can be easily switched on/off by use of solvents.

Results and discussion

The starting polymers [poly-(*R*)-**1** and poly-(*S*)-**1**] are prepared by polymerization of (*R*)- and (*S*)-4-*N*-α-methoxy-α-trifluoromethylphenylacetamides (MTPA) of 4-ethynylaniline [M-(*R*)-**1** and M-(*S*)-**1** respectively]. Poly-(*R*)-**1** and poly-(*S*)-**1** present 3/1 helical structures in non-donor solvents (*e.g.* CH_2Cl_2, $CHCl_3$) with preponderant right-handed [poly-(*R*)-**1**] and left-handed [poly-(*S*)-**1**] helical senses for the backbone frameworks stabilized by intramolecular hydrogen bonds among the *trans* amides of the pendants (Figures 1 and 2).[9]

When a donor solvent (*e.g.* THF) is used to dissolve these polymers, the stereochemistry of the amide bonds change to *cis*, the intramolecular associations disappear by competition of the donor solvent, and as a result the backbone shifts to a more extended 2/1 helix with opposite helical sense, now determined by steric hindrance among pendants (Figures 1 and 2).[9]

The existence of intermolecular interactions between poly-(*R*)-**1** and poly-(*S*)-**1** was evaluated by circular dichroism (CD), dynamic light scattering (DLS) and scanning electronic microscopy (SEM) by using mixtures in different ratios of the starting polymers in THF and $CHCl_3$.

The CD spectra show for all the mixtures and in both solvents signatures corresponding to the contribution of the individual components in the given ratio, indicating that the helical

structures of poly-(*R*)-**1** and poly-(*S*)-**1** remain unaltered (Figure 3a and 3d).

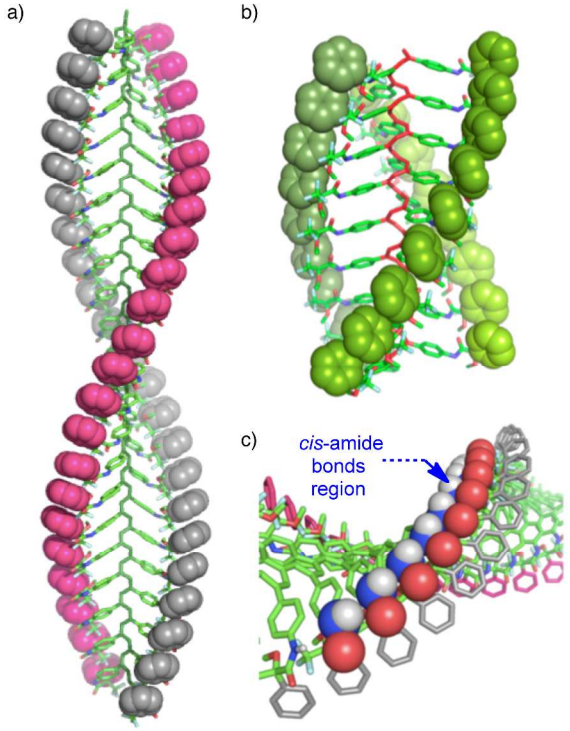

Figure 1. Different helical structures adopted by poly-(*R*)-**1**: a) 2/1 helix (in donor solvents; *cis* pendants) and b) 3/1 helix (in non-donor solvents; *trans* pendants). c) Fragment of the 2/1 helical structure showing the *cis* amide bonds on the crest of the helix.

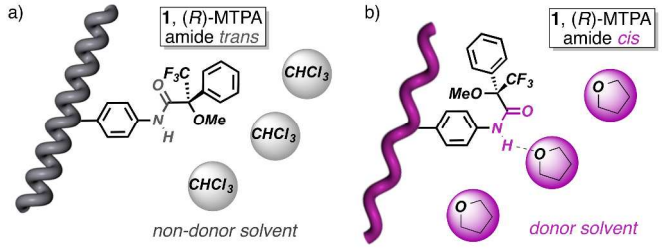

Figure 2. Different helical structures adopted by poly-(*R*)-**1** and the (*R*)-MTPA pendants: a) 3/1 helix (in non-donor solvents; *trans* pendants) and b) 2/1 helix (in donor solvents; *cis* pendants).

DLS traces and SEM images of pure poly-(*R*)-**1** and poly-(*S*)-**1** in both $CHCl_3$ (Figure 3b) and THF (Figure 3e) indicated the formation of polydisperse particles with a diameter around 45 nm. The same type of particles were obtained from the mixture poly-(*R*)-**1**/poly-(*S*)-**1** at a 50/50 (v/v) ratio (Figure 3c) in $CHCl_3$.

In contrast, when this 50/50 (v/v) poly-(*R*)-**1**/poly-(*S*)-**1** mixture was formed in THF, large fiber-like aggregates were observed (Figure 3f).

In contrast, when this 50/50 (v/v) mixture poly-(*R*)-**1**/poly-(*S*)-**1** was made in THF, large fiber like aggregates were observed (Figure 3f).

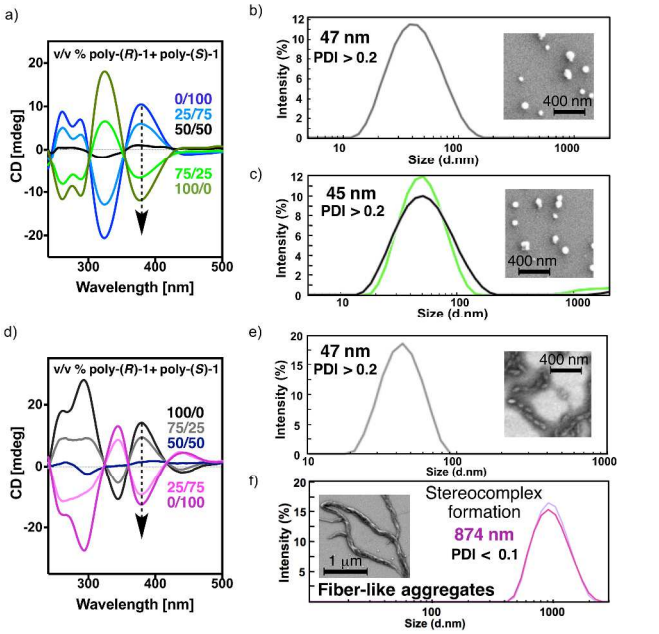

Figure 3. Studies of the stereocomplex formation by CD and DLS: a) CD spectra of different poly-(*R*)-**1**/poly-(*S*)-**1** mixtures in $CHCl_3$ (0.1 mg polymer/mL). DLS traces and SEM images of a solution of b) 100% poly-(*R*)-**1** in $CHCl_3$ (0.1 mg/mL) and c) mixtures of poly-(*R*)-**1**/poly-(*S*)-**1** at 50/50 (v/v) ratio of in $CHCl_3$. d) CD spectra of different poly-(*R*)-**1**/poly-(*S*)-**1** mixtures in THF (0.1 mg polymer/mL). DLS traces and SEM images of a solution of e) 100% poly-(*R*)-**1** in THF (0.1 mg/mL) and f) mixtures of poly-(*R*)-**1**/poly-(*S*)-**1** at a ratio of 50/50 (v/v) in THF.

Similar experiments were carried out with several poly-(*R*)-**1**/poly-(*S*)-**1** mixtures at different ratios. It was found that the presence in the mixture of just 2% v/v of one component [e.g. 20 □L of poly-(*S*)-**1** (0.1mg/mL)/980 □L of poly-(*R*)-**1** (0.1mg/mL)] was enough to induce the formation of supramolecular entities larger than 400 nm (See SI). Moreover, the size of the aggregates can be controlled by the concentration of the starting solutions at any poly-(*R*)-**1**/poly-(*S*)-**1** ratio, becoming larger as the concentration increases (e.g. 50/50 v/v mixtures at 0.05 mg/mL afford 635 nm particles while at 0.5 mg/mL give particles of 1338 nm diameter; see SI).

In summary, these results indicate not only the high specificity but also the effectiveness of the aggregation process that can be triggered by the presence of just 2% of the complementary polymer.

Additional information about the aggregates, the mechanism of the aggregation and the requirements of the starting polymers are described below.

Reversibility of the stereocomplex formation

The structure of the starting polymers poly-(*R*)-**1** and poly-(*S*)-**1** in THF suggests that the helically complementary structures get together by intermolecular association involving hydrogen bonds among the amide groups. If so, temperature changes or the addition of solvents (*e.g.* MeOH) able to disturb hydrogen-bond formation, without interfering with the secondary structure of the polymers (i.e. neither *cis-trans* isomerization nor helical inversion, see pages S28-S31 at SI), should produce

the cleavage of the stereocomplex through intermolecular hydrogen bonding disruption.

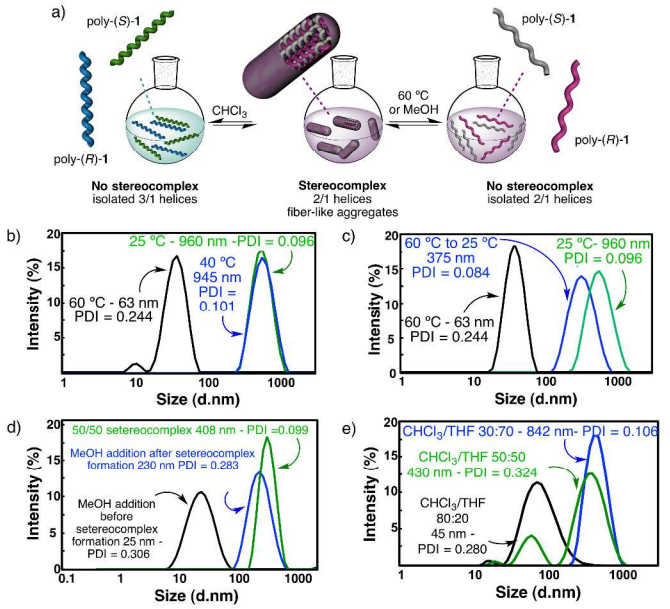

Figure 4. Stereocomplex disruption studies of a poly-(*R*)-**1**/poly-(*S*)-**1** THF solution in a 50/50 (v/v) ratio by DLS. a) Graphical scheme showing the stereocomplex disruption by different external stimuli. b) DLS traces of THF solutions of the stereocomplex at different temperatures: the stereocomplex is stable at 25 ºC and 40 ºC (in green and blue) and is disrupted at 60 ºC (in black). c) DLS traces corresponding to the 50/50 (v/v) poly-(*R*)-**1**/poly-(*S*)-**1** stereocomplex in THF at 25 ºC, at 60 ºC and the recovery of the aggregation after cooling down from 60 ºC (in black) to 25 ºC and stays at that temperature for 1 h (in blue, the stereocomplex is formed again). The original trace of the stereocomplex at 25 ºC (prior to the heating) is shown in green. d) DLS traces showing: the effect of the addition of MeOH to the initial THF solution of poly-(*R*)-**1** before the addition of poly-(*S*)-**1** (formation of the stereocomplex does not take place, in black) and the addition of methanol (in blue, fiber-like aggregates remain in solution) to preformed 50/50 poly-(*R*)-**1**/poly-(*S*)-**1** stereocomplex (in green). e) DLS measurements showing stereocomplex disruption at different $CHCl_3$/THF ratios (30/70, 50/50 and 80/20).

As a matter of fact, DLS analysis of the 50/50 v/v mixture in THF at 60 ºC showed only the presence of isolated polymers indicating that no stereocomplex is present at that temperature (Figure 4b). Furthermore, when the temperature is decreased to room temperature, the stereocomplex is recovered showing the reversibility of its formation in solution (Figure 4c). The size of the recovered stereocomplex after heating at 60 °C is not completely identical to that of the pristine stereocomplex, i.e. from 960 nm (pristine stereocomplex) to 375 nm (recovered stereocomplex).[10] The reassembly among polymer chains after the heating/cooling cycle may not be strictly identical to the previous association since there are assembly points all over the polymer chain that allow a more compact aggregation.

Furthermore, if a hydrogen donor solvent such as methanol is added to the initial THF solution of one of the starting polymers prior to the addition of the other component, the formation of the stereocomplex does not take place because de MeOH is capping the cis-amide hydrogens through hydrogen bond interactions. On the contrary, if the methanol is added to preformed stereocomplex, the fiber-like aggregates are only partially cleaved remaining in solution as smaller size suprastructures (Figure 4d). Finally, if this solution is heated up to 60 ºC the sterecomplexation is disrupted and when the THF/MeOH solution is cooled down the stereocomplex formation does not take place (see a more detailed description of the phenomenon in pages S29-S30 at SI, including Figures S31-S32).

The cleavage of the stereocomplex can be performed not only by heat or by hydrogen bond competition with MeOH but also by addition of solvents that decrease the donor ability of the media. Thus, addition of increasing amounts of $CHCl_3$ to the THF solution of the stereocomplex results in its effective disruption due to the promotion of the *cis*-amide bonds towards the *trans* conformation —the latter involved in intramolecular hydrogen bond interactions— and thus, from a *cis-transoid* 2/1 to a *cis-cisoid* 3/1 helix. Therefore, the intermolecular hydrogen bonds are disrupted (Figure 4e). See a more detailed description of the phenomenon in page S31 at SI, including Figure S33).

All these data indicate that the aggregate is stabilized by hydrogen bonds among *cis* amide groups located at the external parts of the polymer chains. Interestingly, the IR of the poly-(*R*)-**1**/poly-(*S*)-**1** mixture in THF shows the characteristic band for *cis* amides (see SI), identical to the one found in the individual polymers in THF and different from the *trans* band found for the polymers in $CHCl_3$.[9] Therefore, we conclude that the formation of the stereocomplex depends on two factors: *cis* amide functions at the crests of the polymer chains and complementary helices.

Thermal studies on solid phase

Differential scanning calorimetry (DSC) experiments were carried out in order to obtain further information on the thermal properties of the stereocomplex and its secondary structure. This technique has shown to be useful to get information on the thermal isomerizations taking place in this kind of macromolecules [*e.g. cis-transoidal* to *cis-cisoidal (c-t* to *c-c*); *cis-cisoidal* to *trans-transoidal (c-c* to *t-t*)].[11]

Hence, films were prepared from the 50/50 v/v poly-(*R*)-**1**/poly-(*S*)-**1** mixture in THF and in $CHCl_3$ (see SI for experimental procedure), and the DSC traces obtained were compared with those from the parent polymers in the same solvents.

The results revealed identical DSC signatures for the films from poly-(*R*)-**1** and from the poly-(*R*)-**1**/poly-(*S*)-**1** mixture when they are prepared in $CHCl_3$ (Figure 5a). This fact confirms that no new species are being formed when mixing poly-(*R*)-**1**/poly-(*S*)-**1** in that solvent. However, when the same films are prepared in THF, the poly-(*R*)-**1**/poly-(*S*)-**1** mixture shows the *c-t* to *c-c* transition at 147 ºC while the parent poly-(*R*)-**1** exhibit the maximum at 135 ºC. This delay clearly indicates the presence of a new entity, the stereocomplex, different from the

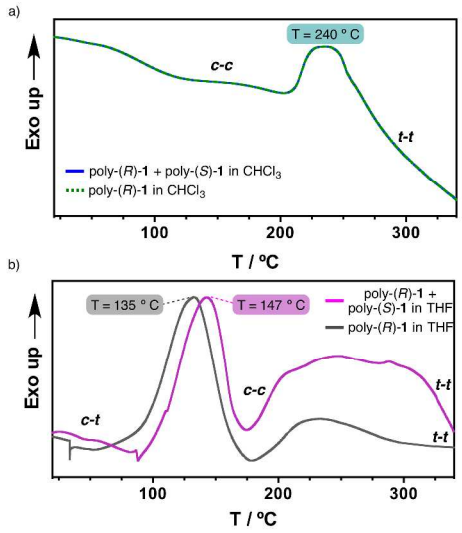

Figure 5. Studies of the 50/50 poly-(*R*)-**1**/poly-(*S*)-**1** stereocomplex disruption by DSC. a) DSC thermograms of poly-(*R*)-**1** and 50/50 poly-(*R*)-**1**/poly-(*S*)-**1** ($CHCl_3$ films). b) DSC thermograms of poly-(*R*)-**1** and the 50/50 poly-(*R*)-**1**/poly-(*S*)-**1** stereocomplex (THF films).

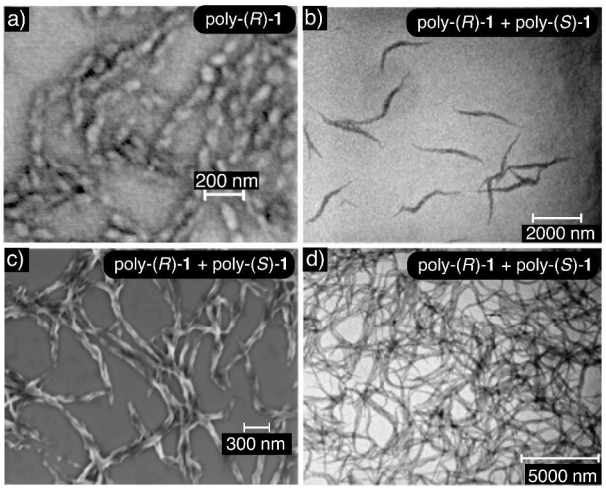

Figure 6. a) SEM images of poly-(*R*)-**1** (concn= 0.1 mg/mL THF) showing nanoparticles (scale bar 200 nm). b) TEM and c) SEM images showing the nanofibers obtained for 50/50 poly-(*R*)-**1**/poly-(*S*)-**1** (concn= 0.1mg/mL THF) (TEM scale bar = 2000 nm, SEM scale bar = 300 nm). d) TEM image showing a gel obtained for 50/50 poly-(*R*)-**1**/poly-(*S*)-**1** (concn= 0.5 mg/mL THF) (scale bar = 5000 nm).

parent polymer, with higher thermal-stability than the starting components (Figure 5b).

Additionally, the first cooling and second heating processes for the poly-(*R*)-**1**/poly-(*S*)-**1** film prepared in THF showed no transition peaks, indicating that both the isomerisation of the backbone and the disruption of the stereocomplex are not reversible under thermal treatment in solid state (see SI).

Electronic Microscopy

Transmission electronic microscopy (TEM) and scanning electronic microscopy (SEM) of poly-(*R*)-**1** and the poly-(*R*)-**1**/poly-(*S*)-**1** stereocomplex confirmed the different nature of the aggregates from both systems: poly-(*R*)-**1** (0.1 mg/mL) in THF showed polydisperse particles of around 45 nm size, in coincidence with the DLS results (Figure 6a), whereas the poly-(*R*)-**1**/poly-(*S*)-**1** mixture (0.1 mg/mL), showed fiber like aggregates (Figure 6b-c). At higher concentrations (0.5 mg/mL), the poly-(*R*)-**1**/poly-(*S*)-**1** stereocomplex evolves from fiber like aggregates to a gel structure (Figure 6d).

Rheology Studies

In order to characterize the gel-like supramolecular structure (Figure 6d), comparative rheological studies were carried out and the results are shown next.

Solutions of the individual polymers [poly-(*R*)-**1** or poly-(*S*)-**1**] in either THF or $CHCl_3$ exhibit viscous behaviour even at 5 mg/mL, with low G'' and negligible G' values (see SI). On the other hand, the rheological parameters of solutions of the 50/50 (v/v) poly-(*R*)-**1**/poly-(*S*)-**1** mixture in THF, revealed a strong dependence on the total concentration. At 0.5 mg/mL, only low G'' values were detected in the stereocomplex solution (see SI). At 2.5 mg/mL the solution presents the typical behaviour of a Maxwell fluid: G'' is larger than G' at low frequencies and increases in a linear fashion with the frequency with a slope close to 2 (see SI). Raising the concentration up to 5 mg/mL, the G'' values become independent of the frequency and the curves of the two moduli show an intersection at 6.28 rad/s; beyond that frequency G' values were greater than G'' (Figure 7a). These results confirm that at high concentrations the stereocomplex behaves as a soft gel. Similarly to what happens in dilute solutions, the on/off switching of the stereocomplex formation can be attained in the gel state by changing temperature and solvent (see Figures S60-S61 at SI).[12]

Finally, as could be expected from the previous CD, SEM and TEM results, similar solutions of the mixture [poly-(*R*)-**1**/poly-(*S*)-**1** at 50/50 (v/v) ratio] in $CHCl_3$ instead of THF, behave as a low viscosity fluid in the whole range of concentrations tested (Figure 7b).

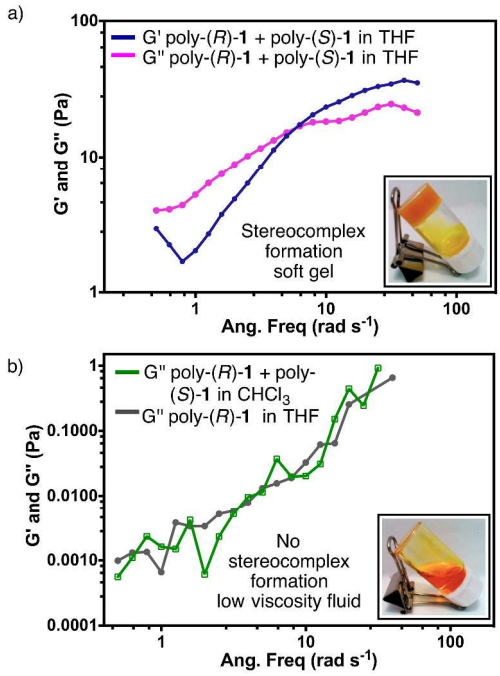

Figure 7. Rheological studies for the (a) stereocomplex in THF (concn= 5mg/mL). b) Comparison between the rheological parameter G'' for a mixture of poly-(*R*)-**1** and poly-(*S*)-**1** in $CHCl_3$ and a solution of poly-(*R*)-**1** in THF (concn= 5mg /mL).

Stereocomplex formation mechanism: Modeling

According to our hypothesis, the formation of the fibers and gel is originated by the aggregation among complementary helices through hydrogen bonds between the *cis* amide groups at the external crests of the polymer chains. In this sense, it became interesting to analyse the geometrical possibilities of that process among polymer chains with the same or opposite helicity and with *trans* and *cis* amide conformation at the pendants.

Geometrical matching of the complementary helices of poly-(*R*)-**1** and poly-(*S*)-**1**, with *cis* amide bonds at the outside (*e.g.* in THF)**,** was studied by computer modeling. The results indicated that interaction between the *cis* amides of those helices is geometrically feasible (Figure 8a), and that the formation of a supramolecular aggregate bound together via multiple hydrogen bonds would be reasonable. On the contrary, if the amides were placed in a *trans* conformation (*e.g.* in $CHCl_3$), no matching between helices is possible, explaining the absence of aggregate. In fact, we tested experimentally other helical poly(phenylacetylene)s with similar geometrical requirements but containing *trans* amides in the external crests, and found no stereocomplex formation. [8d, e]

Moreover, the modeling also showed that no efficient matching could be produced among helices with the same helical sense, even if they present well-placed *cis* amide bonds [*e.g.* right-handed helices of poly-(*R*)-**1** in THF, Figure 8b].

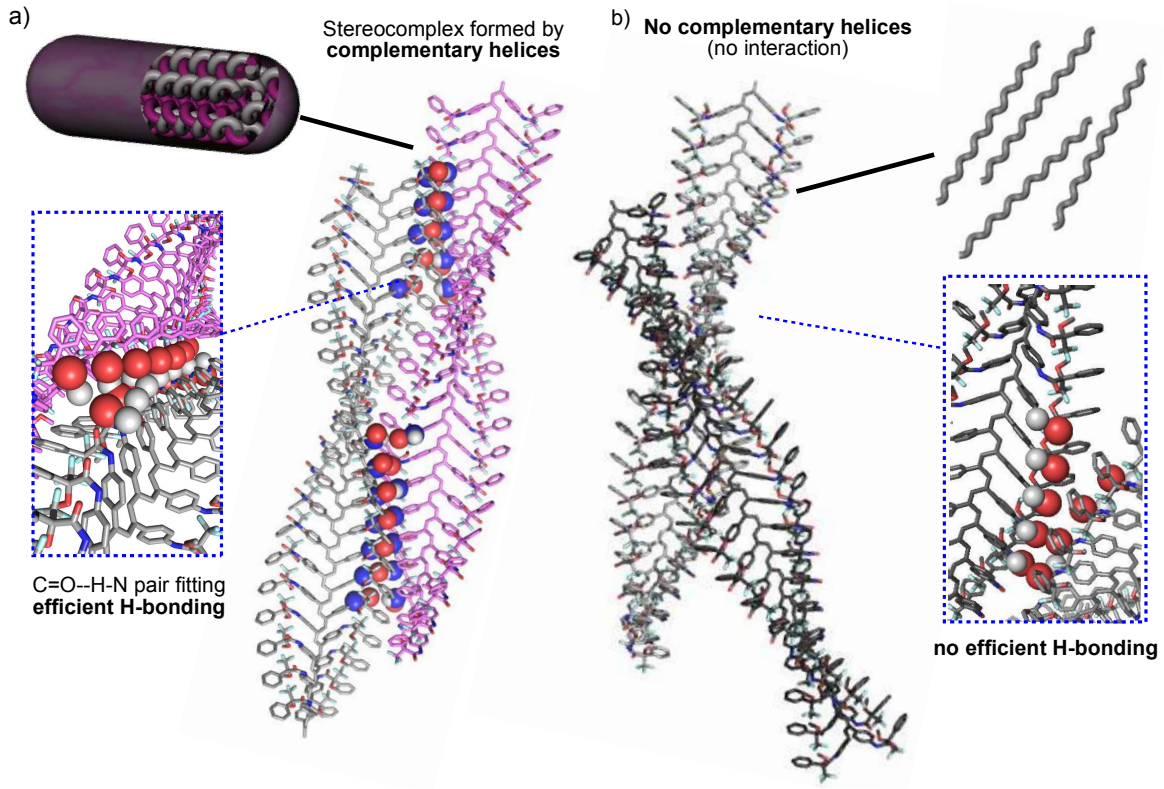

Figure 8. Computer modeling of the complementary helical structures of poly-(*R*)-**1** and poly-(*S*)-**1** forming stereocomplex. b) Computer modelling of the non-complementary helices poly-(*R*)-**1** and poly-(*R*)-**1** (hydrogen bonding interactions are not favoured).

Chemical Science RSCPublishing

ARTICLE

Monitoring stereocomplex formation by AFM

In order to monitor the formation of the stereocomplexes in the solid state, we decided to carefully examine the AFM images obtained during the aggregate formation with mixtures **of** poly-(*R*)-**1**/poly-(*S*)-**1** in THF and to compare them with those of the individual polymers.

Thus, AFM of poly-(*R*)-**1** in THF (0.01 mg/mL) present images of 2D crystals with single right-handed helices packing, and no evidence of large aggregates.[9] However, AFM images of 50/50 v/v poly-(*R*)-**1**/poly-(*S*)-**1** mixture in THF showed, in addition to some isolated 2D-crystals corresponding to the left-handed [poly-(*S*)-**1]** and right-handed [poly-(*R*)-**1]** helices of the individual polymers, the presence of abundant fiber like aggregates. More precisely, fibers with diameters around 3.6 and 5.0 nm are clearly distinguished in addition to higher order fiber aggregates with diameters around 80-100 nm.

The smaller fibers seem to correspond to the initial aggregation steps, and in fact, a width of 3.6 nm fits exactly with the expected one for a dimer (one left handed helix interacting with one right handed helix, Figure 9a). Due to its composition (50/50 mixture of both helices), this dimeric fiber should not present specific helical sense on its surface in full agreement with the experimentally observed AFM (Figure 9a).

As for the fibers with a width of about 4.9–5.0 nm, two different varieties are observed depending on their surface. A first type of those fibers shows no specific helical sense on their surface. This characteristic as well as their width (about 4.9-5nm) fit well with the expected data for a trimer formed by 2 helices of one sense surrounding one helix with the opposite helical sense (Figure 9b).

A second type of fibers was found in the AFM images that present quite similar width as the trimer but with a specific helical sense on its surface (Figure 9c). These data match well with a pentameric structure where one helix chain is surrounded by other four helices of the opposite helical sense. In this case, the fiber surface should reflect the combination of the crests of the four external helices (Figure 9c) and therefore a specific helical sense. Moreover, modeling of this pentameric fiber shows a very good fitting among the individual chains leading to a maximum of about 10.5 nm crest length, in full agreement with the AFM image presented in Figure 9c, where a single helix of poly-(*R*)-**1** is surrounded by four helices of poly-(*S*)-**1**, producing as a result an external left handed helical aggregate.

Naturally, due to the presence of *cis*-amide bonds on the outside crests, these small diameter fiber aggregates (dimer, trimer, pentamer...) can keep growing producing the larger fiber aggregates (about 80-100 nm diameter) that at higher concentrations will afford a gel-like structure (Figures 9d-e).

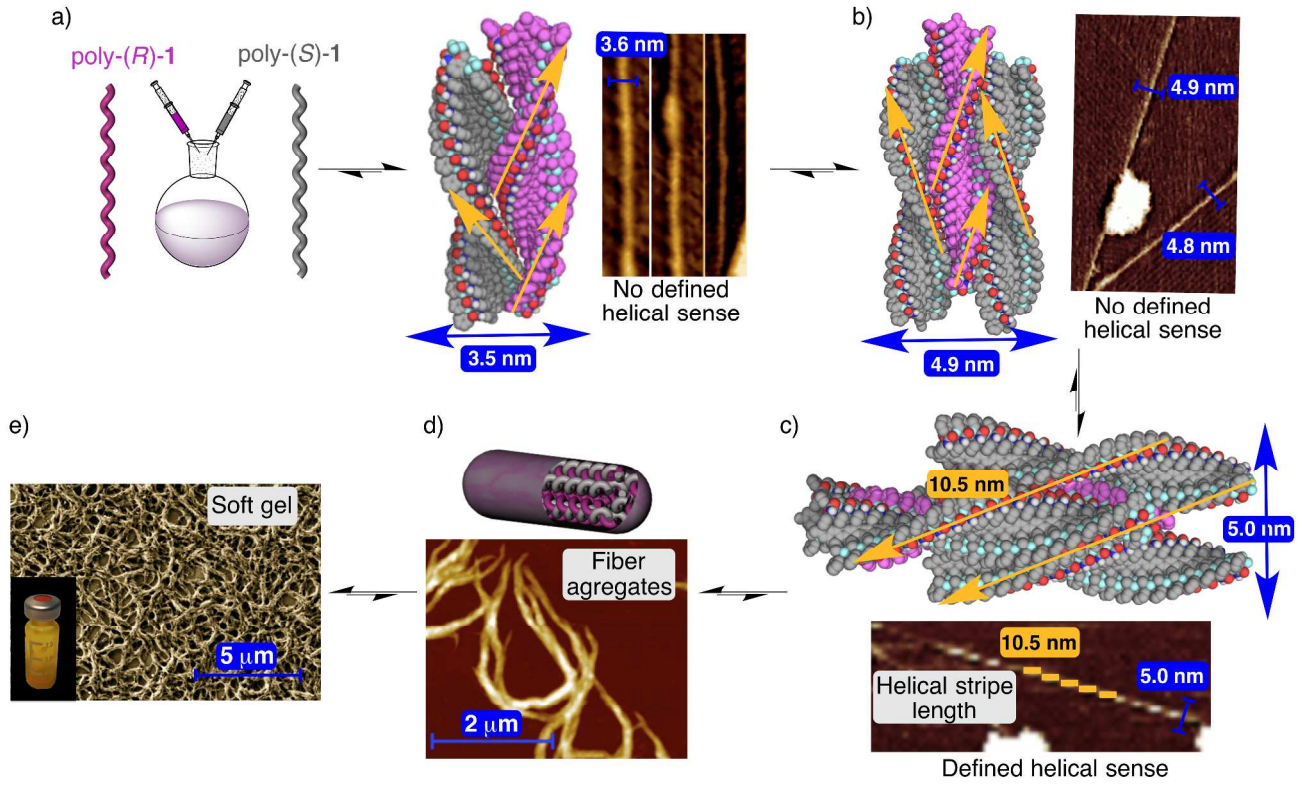

Figure 9. Structure of the stereocomplex. a) Side view of the stereocomplex dimer model (3.5 nm width) and corresponding AFM image showing fibres ≈3.7 nm width. b) Side view of the stereocomplex trimer model (4.9 nm width) and corresponding AFM image showing fibres ≈4.8 nm width. c) Side view of the stereocomplex pentamer model (5.0 nm diameter) and corresponding AFM image showing fibres ≈5.0 nm diameter. d) Conceptual representation of the stereocomplex fiber formation between complementary helices and AFM image showing stereocomplex fiber aggregates. e) Images showing the soft gel structure at microscopic (SEM images) and macroscopic levels (stereocomplex THF solution concn=25 mg/mL). For more detailed depictions, including frontal views of the different types of fibers, see Figures S39-41 at SI.

The effectivity of the binding mechanism: copolymers

Modeling studies indicated that a good geometrical fitting between complementary polymer chains requires the interaction of only a few *cis* amide groups (no more than 6 in a row per helix crest; Figure 8a). Besides that, experimentally we know that addition of just a 2% v/v of one helix to 98% of the complementary one is enough to initiate the aggregation.

To go more deeply into the structural requirements for aggregation, and more precisely, to determine the minimum *cis* amide content in a polymer that is needed for effective aggregation, we decided to prepare copolymers from poly-(*R*)-**1** (or poly-(*S*)-**1**) where some of the units containing *cis* amide at the crests are replaced by similar units containing *trans* amides, and test their aggregation ability.

Thus, copolymers poly-[(*R*)-$\mathbf{1}_{0.9}$-*co*-$\mathbf{2}_{0.1}$] and poly-[(*R*)-$\mathbf{1}_{0.8}$-*co*-$\mathbf{2}_{0.2}$][13] were prepared by copolymerization of M-(*R*)-**1** and M-**2**, [M-**2**= *N*-(4-ethynylphenyl)-2-phenylacetamide], and mixed with poly-(*S*)-**1**. Next, the aggregation was checked by DLS and SEM experiments (Figure 10).

The results indicated that while poly-[(*R*)-$\mathbf{1}_{0.9}$-*co*-$\mathbf{2}_{0.1}$] (10% *trans* amide) is able to form a stereocomplex in the presence of poly-(*S*)-**1** (Figures 10a-c), when the percentage of *trans* amide monomer is increased to reach 20% —poly-[(*R*)-$\mathbf{1}_{0.8}$-*co*-$\mathbf{2}_{0.2}$]—, no stereocomplex is formed by interaction with poly-(*S*)-**1**.

Similarly, the 50/50 mixture of the copolymers poly-[(*R*)-$\mathbf{1}_{0.9}$-*co*-$\mathbf{2}_{0.1}$]/poly-[(*S*)-$\mathbf{1}_{0.9}$-*co*-$\mathbf{2}_{0.1}$] (20% *trans* amide content overall) was found not form stereocomplex (Figures 10d-f) (see full description at SI).

Chemical Science RSCPublishing

ARTICLE

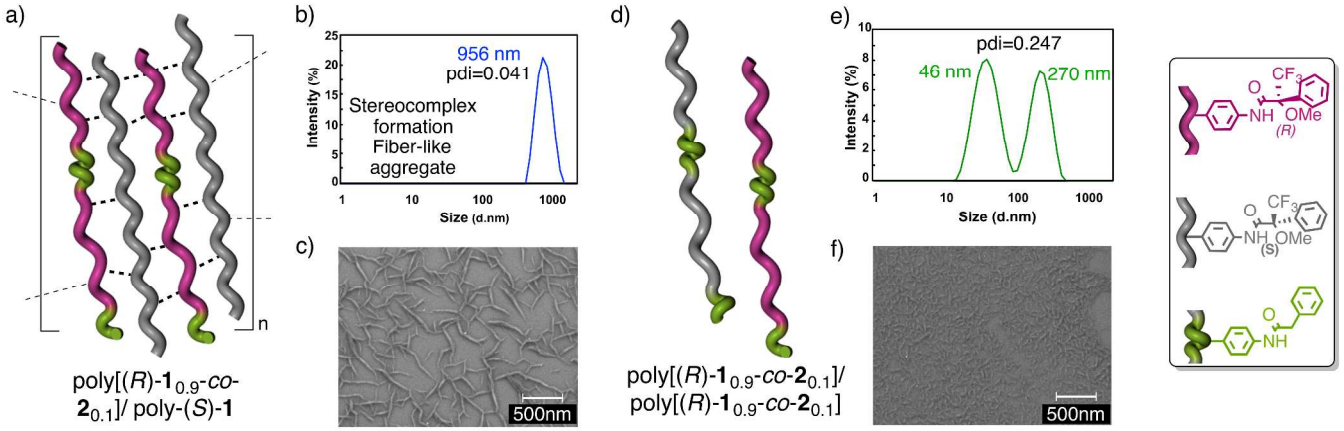

Figure 10. Stereocomplex from copolymer/polymer mixtures. a) Conceptual representation of 50/50 poly-[(*R*)-**1**$_{0.9}$-*co*-**2**$_{0.1}$]/poly-(*S*)-**1** stereocomplex. b) DLS trace of 50/50 poly-[(*R*)-**1**$_{0.9}$-*co*-**2**$_{0.1}$]/poly-(*S*)-**1** stereocomplex. c) SEM image of 50/50 poly-[(*R*)-**1**$_{0.9}$-*co*-**2**$_{0.1}$]/poly-(*S*)-**1** stereocomplex. d) Conceptual representation of the low aggregation showed by 50/50 poly-[(*R*)-**1**$_{0.9}$-*co*-**2**$_{0.1}$]/poly-[(*S*)-**1**$_{0.9}$-*co*-**2**$_{0.1}$] mixtures. e) DLS trace of 50/50 poly-[(*R*)-**1**$_{0.9}$-*co*-**2**$_{0.1}$]/poly-[(*S*)-**1**$_{0.9}$-*co*-**2**$_{0.1}$] mixture. f) SEM image of 50/50 poly-[(*R*)-**1**$_{0.9}$-*co*-**2**$_{0.1}$]/poly-[(*S*)-**1**$_{0.9}$-*co*-**2**$_{0.1}$] mixture.

Conclusions

In this paper we present the first example of a stereocomplex formed by association of helical poly(phenylacetylene)s. The formation of this fiber-like aggregate, that becomes a gel at high concentrations, requires the helical complementarity of the starting polymers and the presence, at the external part of their skeleton, of *cis* amide groups that provide hydrogen bonding to interconnect the helices. The binding and cleavage mechanism, structural and physical properties have been discussed. This is, to our knowledge, the first example of a stereocomplex whose formation can be switched ON and OFF by modulation of the *cis-trans* amide conformation of the pendants.

Acknowledgements

We thank the Servicio de Nanotecnología y Análisis de Superficies (CACTI, UVigo) for recording AFM experiments, and Servicio de Microscopía Electrónica (CACTUS, USC) and Centro de Supercomputación de Galicia (CESGA). We also thank Prof. Dr. Carmen Álvarez-Lorenzo (Dept. Farmacia y Tecnología Farmacéutica, Facultad de Farmacia, USC) for invaluable assistance in the rheology studies.). F. F. also thanks Ministerio de Ciencia e Innovación for a Ramón y Cajal contract.
This work was supported from grants from Ministerio de Ciencia e Innovación [CTQ2009-08632/BQU, CTQ2012-33436, CTQ2012-31381], and Xunta de Galicia (PGIDIT09CSA029209PR, CN2011/037, EM2013/0032

Notes and references

[a] Department of Organic Chemistry and Center for Research in Biological Chemistry and Molecular Materials (CIQUS), University of Santiago de Compostela, E-15782 Santiago de Compostela, Spain. E-mail: felix.freire@usc.es, ricardo.riguera@usc.es.

†Electronic Supplementary Information (ESI) available: [details of any supplementary information available should be included here]. See DOI: 10.1039/b000000x/

1 (a) A. Bertin, *Macromol. Chem. Phys*. 2012, **213**, 2329-2352; (b) J. Slager and A. J. Domb, *Adv. Drug Deliv. Rev*. 2003, **55**, 549-583.
2 (a) H. Tsuji, M. Hosokawa and Y. Sakamoto, *ACS Macro Lett.* 2012, **1**, 687-691; (b) H. Tsuji, S. Yamamoto, A. Okumura and Y. Sugiura, *Biomacromolecules* 2010, **11**, 252-258.
3 T. Kawauchi, A. Kitaura, J. Kumaki, H. Kusanagi and E. Yashima, *J. Am. Chem. Soc.* 2008, **130**, 11889-11891; (b) K. Hatada and T. Kitayama, *Polym. Int.* 2000, **49**, 11-47; (c) R. H. G. Brinkhuis and A. J. Schouten, *Macromolecules* 1992, **25**, 6173-6178; (d) J. Spěváček and B. Schneider, *Adv. Colloid Interface Sci.* 1987, **27**, 81–150.
4 (a) T. Akagi, T. Fujiwara and M. Akashi, *Angew. Chem. Int. Ed.* 2012, **51**, 5493-5496; (b) K. Kondo, T. Kida, Y. Ogawa, Y. Arikawa and M. Akashi, *J. Am. Chem. Soc.* 2010, **132**, 8236-8237; (c) D. Ishii, T. H. Ying, A. Mahara, S. Murakami, T. Yamaoka, W. Lee and T. Iwata, *Biomacromolecules* 2009, **10**, 237-242; (d) Y. Furuhashi, Y. Kimura and N. Yoshie, *Polym. J.* 2006, **38**, 1061-1067; (e) H. Tsuji, *Macromol. Biosci*. 2005, **5**, 569-597.
5 (a) H. Nakayama, T. Manaka, M. Iwamoto and S. Kimura, *Soft Matter* 2012, **8**, 3387-3392; (b) L. Pauling and R. B. Corey, *Proc. Natl. Acad. Sci*. 1953, **39**, 253-256.
6 (a) R. Marín, A. Alla and S. Muñoz-Guerra, *Macromol. Rapid Commun.* 2006, **27**, 1955-1961; (b) I. Iribarren, C. Alemán, C. Regaño, A. Martínez de Ilarduya, J. J Bou and S. Muñoz-Guerra, *Macromolecules*

1996, **29**, 8413-8424; (c) C. Regaño, A. Martínez de Harduya, I Iribarren, A. Rofríguez-Galán, J. A. Galbis, J. A. and S. Muñoz-Guerra, *Macromolecules* 1996, **29**, 8404-8412.

7 For PMMA see: (a) J. Kumaki, S. I. Sakurai and E. Yashima, *Chem. Soc. Rev.* 2009, **38**, 737-746; (b) J. Kumaki, T. Kawauchi, K. Ute, T. Kitayama and E. Yashima, *J. Am. Chem. Soc.* 2008, **130**, 6373-6380; (c) J. Kumaki, T. Kawauchi, K. Okoshi, H. Kusanagi and E. Yashima, *Angew. Chem. Int. Ed.* 2007, **46**, 5348-5351; (d) E. Schomaker and G. Challa, *Macromolecules* 1989, **22**, 3337-3341. For PLA see: (e) H. Marubayashi, T. Nobuoka, S. Iwamoto, A. Takemura and T. Iwata, *ACS Macro Lett.* 2013, **2**, 355-360; (f) P. Pan, J. Yang, G. Shan, Y. Bao, Z. Weng, A. Cao, K. Yazawa and Y. Inoue, *Macromolecules* 2012, **45**, 189-197; (g) J. Zhang, K. Tashiro, H. Tsuji and A. J. Domb, *Macromolecules* 2007, **40**, 1049-1054; (h) J. Zhang, H. Sato, H. Tsuji, I. Noda and Y. Ozaki, *Macromolecules* 2005, **38**, 1822-1828; (i) L. Cartier, T. Okihara and B. Lotz, B. *Macromolecules* 1997, **30**, 6313-6322; (j) D. Brizzolara, H. J. Cantow, K. Diederichs, E. Keller and A. J. Domb, A. J. *Macromolecules* 1996, **29**, 191-197.

8 (a) J. Bergueiro, F. Freire, E. P. Wendler, J. M. Seco, E. Quiñoá, and R. Riguera, *Chem. Sci.* 2014, DOI: 10.1039/C3SC53330A; (b) F. Freire, J. M. Seco, E. Quiñoá and R. Riguera, *J. Am. Chem. Soc.* 2012, **134**, 19374-19383; (c) E. Schwartz, M. Koepf, H. J. Kitto, R. J. M. Nolte and A. E. Rowan, *Polym. Chem.* 2011, **2**, 33-47; (d) F. Freire, J. M. Seco, E. Quiñoá and R. Riguera, *Angew. Chem. Int. Ed.* 2011, **50**, 11692-11696; (e) I. Louzao, J. M. Seco, E. Quiñoá and R. Riguera, *Angew. Chem. Int. Ed.* 2010, **49**, 1430-1433; (f) E. Yashima, K. Maeda, H. Lida, Y. Furusho and K. Nagai, *Chem. Rev.* 2009, **109**, 6102-6211; (g) J. Liu, J. W. Y. Lam and B. Z. Tang, *Chem. Rev.* 2009, **109**, 5799-5867; (h) B. M. Rosen, C. J. Wilson, D. A. Wilson, M. Peterca, M. R. Imam and V. Percec, *Chem. Rev.* 2009, **109**, 6275-6540; (i) T. Sierra, *Expresion of Chirality in Polymers in Chirality at the Nanoscale: Nanoparticles, Surfaces Materials and more*, Chap. 5 (Ed: Amabilino, D. B.), 2009, Wiley-VCH, Weiheim, pp. 115-190; (j) E. Yashima, K. Maeda and Y. Furusho, *Acc. Chem. Res.* 2008, **41**, 1166–1180; (k) E. Yashima and K. Maeda, Chap. 11 (Eds: S. Hecht, I. Huc), Wiley-VCH, Weiheim, 2007, pp. 331-366; (l) K. Maeda, and E. Yashima, *Top. Curr. Chem.* 2006, **265**, 47-88.

9 S. Leiras; F. Freire; J. M. Seco, E. Quiñoá and R. Riguera, *Chem. Sci.* 2013, **4**, 2735-2743.

10 Repetition of the heating/cooling cycle with different batches of polymers yielded analogous results, e.g. 674 nm (PDI= 0.120; pristine stereocomplex) to 460 nm (PDI= 0.190; recovered stereocomplex).

11 (a) A. Motoshige, Y. Mawatari, Y. Yoshida, C. S. Matsuyama and M. Tabata, *J. Polym. Sci., Part A: Polym.Chem.* 2012, **50**, 3008-3015; (b) V. Percec, J. G. Rudick, M. Peterca, M. Wagner, M. Obata, C. M. Mitchell, W. D. Cho, V. S. K. Balagurusamy and P. A. Heiney, *J. Am. Chem. Soc*. 2005, **127**, 15257-15264.

12 The gel formed in THF can be disrupted by addition of a non-donor solvent of lower boiling point such as CH_2Cl_2. After gentle evaporation, the gel state is recovered.

13 See SI for Kellen-Tüdös method.

TOC